Numerical simulations of layered and blended organic photovoltaic cells

J. O. Haerter, S. V. Chasteen, and S. A. Carter[a)]
Department of Physics, University of California, Santa Cruz, California 95064

J. C. Scott
IBM-Almaden Research Center, San Jose, California 95120

We present results obtained from numerical simulations of organic photovaltaic cells as the donor–acceptor morphology evolves from sharply defined layers, to partial blends and finally homogeneous blends. As the mixing percentage increases, the exciton dissociation increases and the diffusion counter-current decreases, resulting in substantially greater short circuit currents but reduced open circuit voltages. Blended structures are more sensitive to mobility than layers due to recombination throughout the bulk. Our model indicates that solar power efficiencies greater than 10% can be achieved when the zero-field charge mobilities approach 10^{-3} cm^2/Vs for partially blended structures. © *2005 American Institute of Physics*. [DOI: 10.1063/1.1901812]

Organic heterostructured photovoltaics have attracted significant interest due to their potential for inexpensively generating electricity. Substantial work has recently been done to simulate numerically layered organic heterojunctions in order to describe the exciton creation and the dissociation at a donor–acceptor (DA) interface, the predominant channel of exciton dissociation.[1–4] Simulations of the optical interference and absorption effects on the exciton generation suggest that the acceptor layer thickness should be chosen approximately as $\lambda/4\eta$ where λ is at the peak of the absorption curve and η is the index of refraction.[3] Further improvements are achieved by minimizing recombination and improving charge collection. Modification of a successful model of charge transport in OLEDs[5] is used to model these effects in layered and blended photovoltaic structures.

Because the exciton diffusion length in organic materials is on the order of 10 nm, the highest performing organic photovoltaics typically involve modification of the organic layers to form partially or fully interpenetrating nanoscale blends. Unfortunately, modeling of blends has proven to be much more difficult than layers due to complications arising from the treatment of the blend morphology and interspecies charge transport. In this letter, we present a model that simulates the performance of a blend of two organic types, either as a homogeneous mixture of two species or a bilayer structure with a partially blended interface layer. This model captures the salient physics of organic-based photovoltaics for a wide range of material morphologies.

The quasi-one-dimensional numerical model considers the absorption and reflection of incident light in blended architectures as well as charge generation and transport within the partially blended bilayer device or homogeneously blended device. For simplicity, we assume only two different species of organic material between emitter and collector, their volume fractions given by $f_1(x)$ and $f_2(x)=1-f_1(x)$. We use glass/ITO/donor/acceptor/Al, where the organic donor and acceptor are taken to have similar properties to the commonly used polymers MEH-PPV and CN-PPV, respectively.

The absorption as a function of position within the device is obtained by the using the Fresnel relations in a trans-

fer matrix method as described previously.[6] The exciton generation rate is then given by:

$$R_{\text{exc}}(x) = \int d\lambda \frac{\lambda}{hc} Q^\lambda(x), \tag{1}$$

with $Q^\lambda(x)$, the time average of the energy dissipated per second at position x and wave length λ, defined by

$$Q^\lambda(x) = \frac{1}{2} c\epsilon_0 \alpha(x)\eta(x)|E(x)|^2, \tag{2}$$

where $\alpha(x)=(4\pi/\lambda)\kappa(x)$, $E(x)$ is the electric field, and $\eta(x)$ and $\kappa(x)$ are the real and imaginary part of the index of refraction $\tilde{n}$, respectively.

Blending at layer interfaces can be caused by mass diffusion into the adjacent organic layer during device construction, leading to a continuous change in $f_i(x)$ as a function of position x that depends on the diffusion constant and the time during which the system interdiffuses. Since neither are known, we present our results by mixing percentage $\Delta = \frac{4}{L}\int_0^{L/2}[1-f_1(x)]dx$ where L is the total thickness of the device. For numerical reasons, we approximate the error function that occurs in the solution of the mass diffusion equation by $\tanh(x)$. The volume fraction is therefore given by:

$$f_1(x) = \frac{1}{2}\{1 - \tanh[(x - x_i)/\delta_b]\}, \tag{3}$$

and $f_2(x)=1-f_1(x)$ where x_i is midpoint of the blended region and δ_b specifies the blend width, with $\delta_b\to 0$ for layers and $\delta_b\to\infty$ for homogenous blends. For blended structures, the complex index of refraction $\tilde{n}(f_1(x),\lambda)$ is a continuous function of position, as given by the ratio $f_1(x)/f_2(x)$ of the two species. The concentration dependent index of refraction is determined from effective medium theory[7] via the Bruggeman formula $\epsilon=\frac{1}{4}(\beta+\sqrt{\beta^2+8\epsilon_1\epsilon_2})$ for the effective dielectric constant ϵ of a mixture of two species where $\beta=(3f_1-1)\epsilon_1+(3f_2-1)\epsilon_2$, and ϵ_1 and ϵ_2 are the respective complex dielectric functions of the two species. In the case of a continuous change of $\tilde{n}$ as function of x, a separate layer and interface matrix is defined for every cell of width 0.5 nm. The resulting values $\tilde{n}(x)=\epsilon^{1/2}(x)$ then enter Eq. (2).

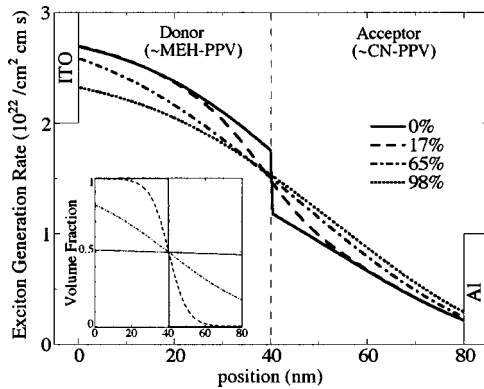
a)Electronic mail: sacarter@ucsc.edu

FIG. 1. Exciton generation rate vs position for different mixing percentages. Inset: volume fraction of species f_1 as a function of position; $f_2(x)=1-f_1(x)$.

For an incident solar light intensity of 100 mW/cm^2, we compute the exciton generation rate as a function of position within the device, as shown in Fig. 1. A thickness of 40 nm has been chosen since it roughly corresponds to $\lambda/4\eta$ for the acceptor index of refraction η. In the case of $\delta_b=0$, the graph exhibits a sharp drop in R_{exc} at the layer–layer interface due to the higher absorption coefficient of the donor material. A very low rate of exciton generation occurs at the highly reflecting Al cathode. For increasing mixing percentage, the sharp discontinuity at the interface gradually smoothens out. The decline of R_{exc} near the anode and an increase near the cathode are due to the change in the index of refraction resulting from the mixing of the two species.

Due to the large exciton binding energy in organic materials, exciton dissociation takes place predominantly at interfaces of materials with differing molecular orbital energies.[1] For the layers, only excitons created within the exciton diffusion length of the donor–acceptor interface are allowed to dissociate. Excitons in the blended region are assumed to dissociate if they are created within a diffusion length of the range of x where the concentration of both phases exceeds the percolation threshold.

For each mixing percentage, we first integrated over position to determine the total number of excitons created within the device. Assuming that every exciton within the range of a dissociation site yields a free electron and a free hole that arrive at the contacts, we computed the theoretical maximum limit for the current density obtained from this model (Fig. 2). In the case of layers, only a small fraction of
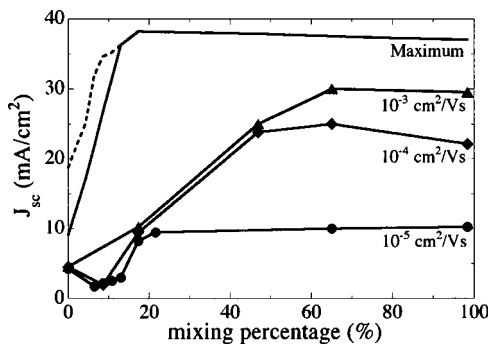

FIG. 2. Short circuit current, J_{sc}, as a function of mixing percentage for different zero-field carrier mobilities. Maximum line assumes all excitons generated are collected, with $L_{exc}=10$ nm (all solid lines) and $L_{exc}=20$ nm (dashed line).

the total excitons created has a chance to dissociate. The total number of dissociated excitons almost doubles for double exciton diffusion length L_{exc} (dashed line). With increasing mixing percentage, a larger volume contributes to the dissociated excitons, thus we find an increase in the maximum current density. For mixing percentages past the percolation threshold of 18%, the maximum current decreases slightly due to the smaller fraction of the more strongly absorbing donor material close to the anode.

Once the excitons dissociate, we simulate the charge transfer and transport processes using the numerical model developed to describe charge transport in layered organic light-emitting diodes.[5] We first compute the thermionic injection current densities[8] for the two species individually and then weight these with the factors $f_i(x)$. This will lead to an injection of charges into species 1 and species 2. The boundary condition is given by the difference of the externally applied voltage and the difference in work functions of the contacts, namely ITO (4.8 eV) and aluminum (4.2 eV). The currents and the electric field are specified at the cell–cell interfaces, whereas the charge densities and the mobilities are specified at cell centers. The steps in chemical potential due to the internal layer interfaces are taken into account by a Miller–Abrahams form.[5]

For transport in the blends, we retain the quasi-one-dimensional model in which currents and charge densities are a function of distance from the anode contact. For simplicity, no change in mobility above the percolation threshold is assumed. We determine the percolation threshold, namely the critical volume fraction of the species at which a continuous pathway occurs, by modeling the polymer materials as spherical blobs of equal radius.[9,10] Below the percolation threshold, charges are able to make interspecies but not intraspecies transitions. Transfer between phases is allowed at every given position x and the mobility within the same phase depends linearly on the concentration of that phase. The likelihood for a charge carrier to encounter species i is determined by its fraction in the whole material. This yield four equations:

$$J_{e,ij}(x) = f_i(x)f_j(x+\delta x)e\mu_e(x,E)n(x)E(x) + D(\mu)\frac{dn(x)}{dx},$$

(4)

where the charge density $n(x)$ is now taken to be the average of the charge densities $n_i(x)$ and $n_j(x+\delta x)$ and by $dn(x)/(dx)$ we now mean $n_j(x+\delta x)-n_i(x)/(\delta x)$. The mobility $\mu_e(x,E)$ is the average mobility $1/2[\mu_{e,j}(x+\delta x,E)+\mu_{e,i}(x,E)]$ and the mobilities are field dependent through $\mu_e(x,E)=\mu_e^0 \exp(\gamma_e\sqrt{E})$ and μ_e^0 is the zero-field mobility. These equations apply analogously to the hole currents. The steps in the chemical potential due to the internal interfaces between different species are taken into account by a Miller–Abrahams form.[5] For electrons, this means that if $J_{e,ij}(x)\Delta\mathcal{E}<0$ where $\Delta\mathcal{E}=\mathcal{E}_i(x)-\mathcal{E}_j(x+\delta x)$ then the electron current $J_{e,ij}$ as computed from the drift-diffusion equation Eq. (4) is replaced by $\exp(-\beta\Delta\mathcal{E})J_{e,ij}$. The parameters entering the simulation are given in Table I.

Using these equations and parameters, we compute the mobility-dependent short circuit current J_{sc}, shown in Fig. 2. In blends, the ability of the charges to change phase at every position x and thus recombine means that higher mobilities result in a greater chance that the carriers can exit the device

TABLE I. Parameters used in the simulation for $T = 300$ K.

	Donor	Acceptor
HOMO (eV)	5.3	5.9
LUMO (eV)	3.0	3.5
$\mu_e^0/\mu_h^0 (10^{-6}$ cm^2/V s)	1–100/10–1000	10–1000/1–100
$\gamma_e/\gamma_h [10^{-4} (\text{m/V})^{1/2}]$	5/5	5/5
L_{exc}(nm)[a]	10	10
Thickness (nm)	40	40

[a]Exciton diffusion length.

before recombination. In a layered structure, the sharp interface leads to separate charge pathways so that higher mobility does not significantly affect recombination. The best performance is observed for moderate mixing percentages that enable direct pathways between the contacts and dissociation sites throughout the device while reducing the area that enables interphase transfer of the charges and thus the opportunities for recombination.

Finally, we generated *J–V* curves for several blend widths and mobilities and from these computed the fill fac-
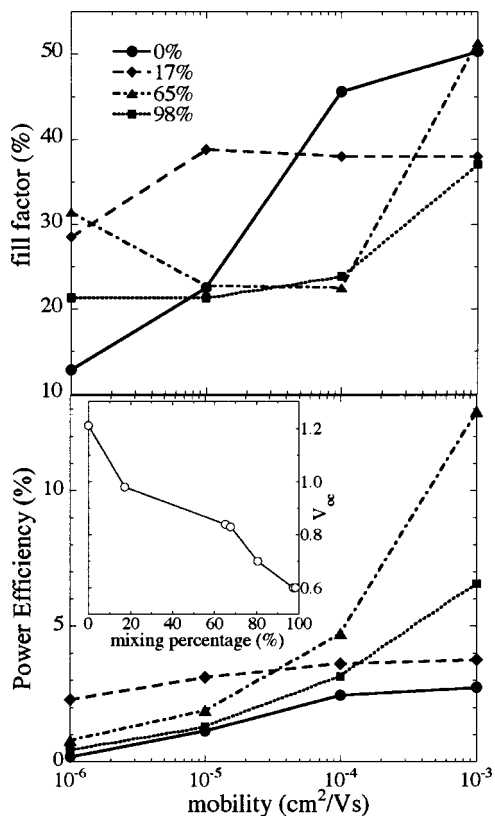

FIG. 3. Fill factor (top) and power efficiency under solar conditions (bottom) as a function of zero-field carrier mobilities for different mixing percentages. Inset: open-circuit voltage (V_{oc}) vs mixing percentage.

tor, open circuit voltage and the power efficiency, as shown in Fig. 3. In general, FF increases with increasing mobility for low mixing percentage, but more blended devices show fairly low FF ($\approx 23\%$) until large mobilities are reached. V_{oc} shows clear dependence on blending. Largest V_{oc} is gained for layers and drops to the value of the built-in potential for homogeneous blends. This effect is caused by a reduction in the diffusion current in blends caused by the formation of a continuous pathway between electrodes.[1,2] For high mobilities, we observe a linear dependence of the power efficiency on light intensity, but expect sublinear behavior as space charge effects become appreciable at lower mobilities. These results are in reasonable quantative agreement with experiments on MEH-PPV/CN-PPV and related heterostructured photovoltaics.[4,11–13]

In conclusion, we have presented a model that can simulate the response of a blended photovoltaic device to incident solar light. This model is readily extended to a wide range of organic morphologies. Our results indicate that the best performing devices have a partially blended donor–acceptor morphology. For zero-field mobilities approaching 10^{-3} cm^2/Vs, power efficiencies above 10% were observed. These results suggest that polymer/polymer blended photovoltaics can achieve high power efficiencies if the mobility can be moderately increased for both carriers and the partially blended morphology can be controlled via mass diffusion, even with the absorption properties of currently existing materials.

[1]B. A. Gregg, J. Phys. Chem. B **107**, 4688 (2003).
[2]J. A. Barker, C. M. Ramsdale, and N. C. Greenham, Phys. Rev. B **67**, 075205 (2003).
[3]P. Peumans, A. Yakimov, and S. R. Forrest, J. Appl. Phys. **93**, 7 (2003).
[4]S. V. Chasteen, J. O. Haerter, G. Rumbles, J. C. Scott, and S. A. Carter, Phys. Rev. B (submitted).
[5]B. Ruhstaller, S. A. Carter, S. Barth, H. Riel, W. Riess, and J. C. Scott, J. Appl. Phys. **89**, 8 (2001).
[6]L. A. A. Pettersson, L. S. Roman, and O. Inganas, J. Appl. Phys. **86**, 1 (1999).
[7]T. C. Choy, Effective Medium Theory, p. 13 (1999).
[8]J. C. Scott and G. G. Malliaras, Chem. Phys. Lett. **299**, 115 (1999).
[9]H. Scher and R. Zallen, J. Chem. Phys. **53**, 3759 (1970).
[10]M. J. Powell, Phys. Rev. B **20**, 4194 (1979).
[11]J. J. M. Halls, C. A. Walsh, N. C. Greenham, E. A. Marseglia, R. H. Friend, S. C. Moratti, and A. B. Holmes, Nature (London) **376**, 498 (1995).
[12]M. Granstroem, K. Petritsch, A. C. Arias, A. Lux, M. R. Andersson, and R. H. Friend, Nature (London) **395**, 257 (1998).
[13]A. J. Breeze, Z. Schlesinger, S. A. Carter, H. Tillmann, and H. H. Hoerhold, Sol. Energy Mater. Sol. Cells **83**, 263 (2004).